POLITECNICO
MILANO 1863

SCUOLA DI INGEGNERIA INDUSTRIALE
E DELL'INFORMAZIONE

Executive Summary of the Thesis

Numerical modelling of cardiac perfusion with application to aortic valve stenosis

Laurea Magistrale in Mathematical Engineering - Ingegneria Matematica

Author: Martina Falasca

Advisor: Prof. Luca Dede'

Co-advisor: Michele Bucelli, Alberto Zingaro

Academic year: 2023-2024

1. Introduction

Cardiovascular diseases (CVDs) are the world's leading cause of death, accounting for approximately 17.9 million deaths each year. This number is expected to grow to more than 23.6 million by 2030. The increasing impact of CVDs worldwide has been one of the main drivers that have made the mathematical and numerical modelling of the cardiovascular system a field of great interest for the scientific community in the past 25 years [4]. Within the CVDs, valvular heart diseases (VHDs) represent the leading cause of cardiovascular mortality, with aortic valve stenosis (AS) being one of the most common diseases in western countries. Given that age represents a significant risk factor for AS, late treatments significantly increase the mortality rate. For this reason, an accurate diagnosis becomes essential for the effective treatment of the disease and computational studies can assist in achieving this. On top of that, the pathology frequently leads to complications in myocardial perfusion [2], that is the complex process by which oxygenated blood is delivered to the myocardium, enabling its oxygenation and metabolism [5]. In some cases, this can lead to coronary artery diseases and symptoms of angina. In this context, the objective of this thesis is to conduct a comprehensive analysis of a multiphysics computational model for human cardiac perfusion, proposed in [5], and to investigate its application to the case of AS. The model accounts for electromechanics, fluid mechanics, valve modeling and perfusion. This work is carried out in two stages. First, starting from the model setup in [5], we inspect the reliability of the model in describing cardiac perfusion in a healthy scenario. Then, we apply the model to the AS case, creating a three-dimensional obstruction of the flow field across the aortic valve. We aim to investigate how the model is able to predict the effects of the pathology on myocardial perfusion. To the best of our knowledge, this work represents the first attempt in the literature to include AS into a multiphysics model of the cardiac function that considers the entire anatomy of the left heart.

2. Mathematical models and numerical methods

Starting from the model setup in [5], we employ a comprehensive multiphysics model of human cardiac perfusion, based on the coupling

between the Navier-Stokes equations in ALE configuration for the hemodynamics and the three-compartments Darcy equations for the intramural vessels. The model is driven by a fully coupled electromechanical model of the left heart and incorporates the multiscale and multiphysics features of myocardial perfusion by describing the hemodynamics inside the left heart and the coronary arteries and accounting for the intramural vessels by modelling the myocardium and its microvasculature as a porous medium. The coupling between the two models in set by enforcing mass conservation and the balance of internal forces at the interfaces between fluid dynamics and perfusion domains. The cardiac valves are modeled by means of the Resistive Immersed Implicit Surface (RIIS) method. We consider two different spatial domains: the fluid problem is set in the left heart fluid domain Ω^{f}, that consists of the left ventricle and atrium chambers, the aorta and the epicardial coronaries, while we solve the perfusion problem in a biventricular geometry Ω^{p}. For the numerical distrectization of the fully coupled problem we employ Finite Difference Schemes for the discretization in time, using a first order Backward Difference Formula (BDF1), while, for the spatial discretization we use the Finite Element Method (FEM). Regarding the fluid problem, we use linear FE spaces ($\mathbb{P}^1 \setminus \mathbb{P}^1$) for both the fluid velocity and pressure, with a VMS-LES stabilization, that acts also as a turbulence model. Moreover, we treat the non linear convective term of the Navier-Stokes momentum equation in a semi-implicit way.

3. Computational setup

The geometries of the computational domains Ω^{f} and Ω^{p} are defined starting from the Zygote solid 3D heart model, an anatomically CAD model of an average healthy human heart. Starting from the model setup in [5], we consider a tetrahedral mesh for the computational domain Ω^{f} and an hexaedral mesh for Ω^{p}. The fluid dynamics mesh is refined near the valves leaflets, in order to accurately capture them with the RIIS method. Regarding the fluid problem, the density and the dynamic viscosity of the fluid are considered to be constant and taken from the literature, namely: $\rho = 1.06 \cdot 10^3\,\mathrm{kg/m^3}$ and $\mu = 3.5 \cdot 10^{-3}\,\mathrm{kg/(ms)}$. We let the valves open and close instantaneously, at the initial and final times of isovolumetric phases. Concerning the multi-compartment Darcy problem, following the setup of the model discussed in [3], the computational domain Ω^{p} is divided into seventeen perfusion regions, one for each terminal vessel. The calibration of the Darcy parameters is performed as in [3, 5].
We start our simulations at the end of the filling phase. We simulate two heartbeats and we report the solutions of the second cycle, in order to reduce the influence of a non-physical null velocity as initial condition [5]. For the numerical solution of the fully coupled problem, we use an implicit method with an iterative splitting strategy, dividing the problem into two sub-problems that are solved sequentially. The associated linear systems are solved at each time step with the GMRES method. We perform the numerical simulations in `life`$^{\mathrm{x}}$ [1], a high-performance Finite Element library, mainly focused on cardiac simulations. The numerical simulations are run in parallel on 56 cores, with a computational time of about 60 hours.

4. Test I: physiological simulation

In the first part of our study, we successfully replicate a healthy simulation scenario. Regarding the calibration of the parameters, we investigate the RIIS resistance R_k and the half thickness ϵ_k, $k \in \{\mathrm{MV}, \mathrm{AV}\}$, for the aortic and mitral valves, and the timesteps. The choice of the RIIS parameters not only affects the physical structure of the valves, but also influences the condition number of the linear system associated to the FE discretization of the fluid problem. It is observed that the condition number of the system becomes larger as $\frac{R_k}{\epsilon_k}$ increases. For this reason, we calibrate the parameters R_k and ϵ_k, taking into account their ratio. Moreover, we select ϵ_k as to obtain an aortic valve orifice area compatible with the values of healthy valves observed in the literature. Finally, when calibrating R_k, we aim to minimize flow penetration across the leaflets. Table 1 reports the values of the RIIS parameters used in the simulation, while Figure 1 displays the cardiac valves employed in the simulation in the open and closed configuration. Following the model setup in [5], we perform the simulation with a timestep of

$\Delta t = 5 \cdot 10^{-4}$ s for both the fluid dynamics and the multi-compartment Darcy simulation.

Parameter	Value
ϵ_{AV}	$2 \cdot 10^{-3}$ m
ϵ_{MV}	$2 \cdot 10^{-3}$ m
R_{AV}	$1 \cdot 10^{4}$ kg/(m s)
R_{MV}	$1 \cdot 10^{4}$ kg/(m s)

Table 1: RIIS parameters employed in Test I .

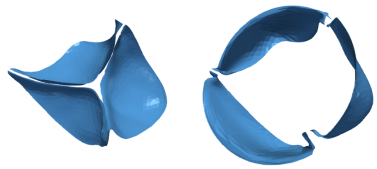

(a)

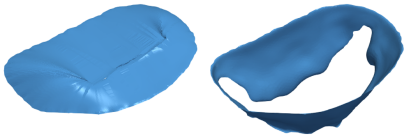

(b)

Figure 1: Valves in the open and closed configuration: (a) aortic valve; (b) mitral valve.

We inspect the physiological reliability of the model by comparing some relevant biomarkers obtained by the physiological simulation against clinical ranges coming from the literature. We compute the left ventricular stroke volume and the ejection fraction equal to 82 ml and 52.3%, respectively, values that are consistent with the clinical ranges. Regarding the fluid dynamics in the left heart domain, we investigate the blood flow rates inside the ascending aorta, the pulmonary veins and the coronary arteries. We also examine the pressures inside the aorta and the coronary arteries, values that strongly influence myocardial perfusion. Coherently with physiological data, the flow rate at the aortic outlet section reaches the peak value of 562 ml/s during systole, while in the pulmonary veins a peak total flux of 267.2 ml/s is reached during diastole. Furthermore, the flowrate profiles inside the coronaries are in accordance with clinical evidences: at the beginning of diastole a peak blood flow rate is observed for both the fluxes computed at the outlet sections of the left coronary artery (LCA) and of the right coronary artery (RCA), that is coherent with the coronary blood flow behavior in response to the myocardium contraction and relaxation. We measure a larger flux in the LCA than the one in the RCA, as expected. Finally, we observe physiologically consistent pressure profiles and we measure values for the systolic peak and the diastolic minimum of the pressure inside the ascending aorta equal to 103.3 mmHg and 80.3 mmHg, respectively, both results consistent with the clinical data [5]. From the multi-compartment Darcy simulation we obtain the pressures in the three Darcy compartments. The pressures decrease from the first compartment going to the last one, but present comparable values during the systolic peak due to the partial obstruction of the vessels resulting from the myocardial contraction, as expected.

5. Test II: aortic valve stenosis simulation

In the second numerical simulation we apply the multiphysics model to the case of AS. To this purpose, we reduce the aortic valve displacement by 60 % modifying the displacement filed of the healthy valve, in order to reduce the orifice area. Figure 2 shows the stenotic aortic valve employed in this simulation, as well as a comparison with the healthy one in the open configuration, highlighting the different orifice areas. Moreover, we recalibrate ϵ_{AV}, in order to replicate a scenario corresponding to a severe pathology. To ensure physiological consistency between the two valves, the same thickness is introduced for the mitral valve. Furthermore, in order to avoid spurious flow across the valves leaflets, we increase the valves resistance R_k and we introduce a scaling factor for the parameter ϵ_k, whereby the valves are doubled in thickness within the closed configuration, returning to the half thickness employed in Test I. Table 2 reports the value of the RIIS parameters used in the simulation.

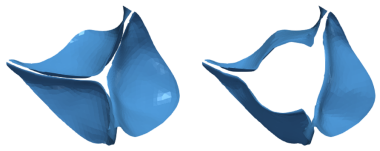

(a)

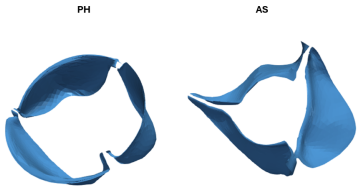

(b)

Figure 2: Representation of the stenotic valve employed in Test II: (a) stenotic aortic valve in the open and closed configuration; (b) physiological aortic valve (PH) versus stenotic aortic valve (AS) in the open configuration.

Parameter	Value	
	Open configuration	**Closed configuration**
ϵ_{AV}	$1 \cdot 10^{-3}$ m	$2 \cdot 10^{-3}$ m
ϵ_{MV}	$1 \cdot 10^{-3}$ m	$2 \cdot 10^{-3}$ m
R_{AV}	$5 \cdot 10^{4}$ kg/(m s)	$5 \cdot 10^{4}$ kg/(m s)
R_{MV}	$5 \cdot 10^{4}$ kg/(m s)	$5 \cdot 10^{4}$ kg/(m s)

Table 2: RIIS parameters employed in Test II.

Finally, we reduce the timestep by half, namely $\Delta t = 2.5 \cdot 10^{-4}$ s. The reason for this is to avoid numerical instabilities, that can arise due to the increase of the $\frac{R_k}{\epsilon_k}$ ratio, as discussed in Section 4. We test the model by comparing several biomarkers obtained from the simulation with the ranges in the clinical literature and with the results obtained from Test I. Our results show that the model successfully predicts the flow across the stenotic aortic valve as a flow through a convergent orifice. As shown in Figure 3, the blood flow across the stenotic valve accelerates and gets more skewed and narrower, with respect to the healthy case, which is uniform and evenly distributed across the aorta. Moreover, the model faithfully predicts the generation of a vortex ring at the extremity of the blood jet, and the subsequent development of a recirculation region in proximity of the aortic sinus. The comparison demonstrates that the blood flow across the stenotic valve predicted by the model is in accordance with clinical evidences.

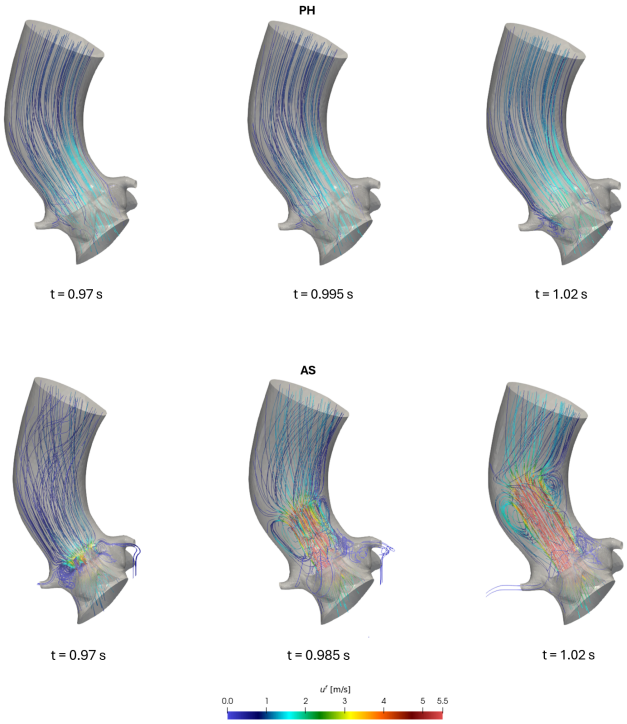

Figure 3: Comparison between velocity field inside the ascending aorta during systole obtained in Test I (PH) and Test II (AS). Four different frames from t=0.97 s to t=1.02 s are reported.

Moreover, we observe that while the pressure downstream the ascending aorta recovers the physiological profile, the average pressure in the coronary sinus exhibits notable oscillations around the pressure values measured at the aortic outlet section, in contrast to Test I. This is consistent with the emergence of a recirculation region slightly downstream of the stenotic valve. Regarding the coronary pressure, it can be observed that both the LCA and RCA curves exhibit a peak at the beginning of systole, that we deem is consistent with the pressure profiles inside the ascending aorta. The coronary pressures measured in Test II during systole are higher than those observed in Test I, but then revert to the physiological profile observed in Test I during diastole. In Figure 4, we compare the coronary flow rates of Test I and Test II. It

can be observed that both the flowrate in the LCA and in the RCA increase during systole with respect to Test I, while during diastole the curves tend to recover the physiological values. We deem that the coronary flow rates observed in Test II are the consequence of the pressure curves discussed above. In particular, we believe that the high pressure fluctuations observed in the coronary sinus at the beginning of systole cause an initial acceleration of the the blood flow inside the coronaries, thereby increasing the flow rate during systole.

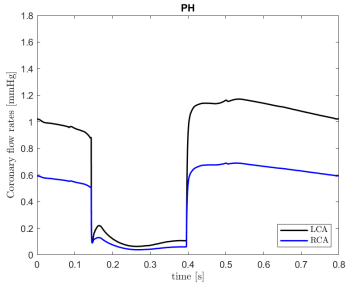

(a)

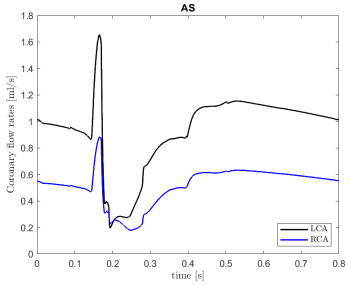

(b)

Figure 4: Flow rates in epicardial coronary arteries outlet sections in a representative heartbeat: (a) Test I; (b) Test II.

Furthermore, we investigate the spatial distribution of the pressure in the fluid domain. As illustrated in Figure 5, during systole the pressure in the left ventricle reaches higher values in Test II, compared with Test I, due to the obstruction of the outgoing flow, as expected, while the pressure field during diastole exhibits the same values that are obtained in Test I.
Finally, we examine the pressures in the biventricular geometry, that are shown in Figure 6. It is observed that the pressure inside the first and second Darcy compartments exhibits a profile that correlates with the pressure profiles observed in the coronary arteries, whereas the pressure within the third compartment lies in a range of values that is consistent with the ones measured in Test I.

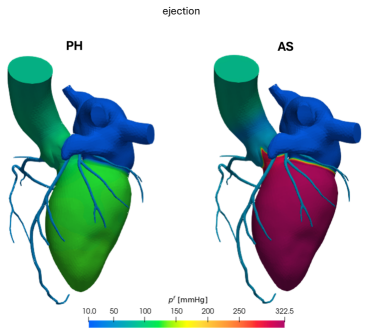

(a)

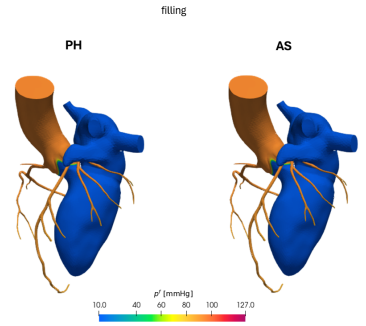

(b)

Figure 5: Pressure on the boundary of Ω^f, comparison between Test I and Test II during ejection and filling phases: (a) ejection ($t = 1$ s); (b) filling ($t = 1.45$ s).

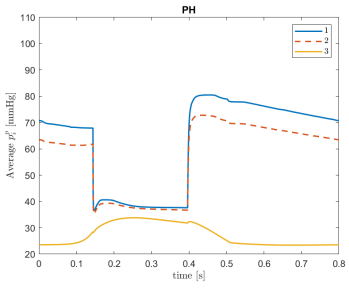

(a)

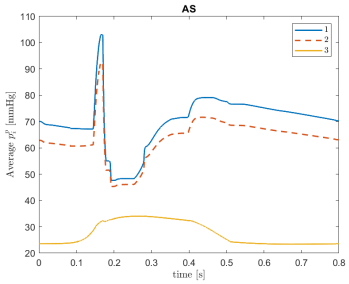

(b)

Figure 6: Pressure in the three Darcy's compartments in a representative heartbeat: (a) Test I; (b) Test II.

6. Conclusions

In this work, we analyzed in detail a mathematical model for human cardiac perfusion, showing its reliability in simulating myocardial perfusion in both healthy and AS conditions. In the first part of our study, we successfully inspected the model biophysical fidelity in a healthy scenario, comparing several biomarkers obtained by our simulation against clinical ranges coming from the literature. We then applied the model to the case of aortic valve stenosis. To this purpose, we performed a recalibration of the parameters of the model along with a reduction of the aortic valve displacement, in order to obtain a valve orifice area which corresponds to a scenario of a moderate to severe aortic valve stenosis. We reduced the aortic valve thickness, in order to replicate a scenario corresponding to the pathology. To ensure physiological consistency between the two valves, the same thickness was introduced for the mitral valve. To avoid spurious flow across the valves leaflets, we increased the valves resistance and doubled the valves thickness when in closed configuration. Furthermore, in order to avoid numerical instabilities, the time steps were reduced in comparison to the healthy configuration. Our results showed that the model successfully predicts the flow across the stenotic aortic valve as a flow through a convergent orifice. We indeed observed that the blood flow across the stenotic valve accelerates and gets more skewed and narrower, with respect to the healthy case. Moreover, the model faithfully predicts the generation of a vortex ring at the extremity of the blood jet, and the subsequent development of a recirculation region in proximity of the aortic sinus. Furthermore, we assessed that the model is able to capture changes in the coronary flow due to the three-dimensional obstruction of the flow field across the aortic valve, since the coronary flowrates and pressure in the pathological case show different profiles than the healthy simulation.

The major limitation in this thesis is in the use of the same displacement filed for both the healthy and pathological simulations. This lead us to neglect the effects of the stenosis on the left ventricle. Moreover, the calibration of the mesh size was performed considering the valves configuration in the healthy simulation. In the pathological simulation, we diminished the valves thickness and consequently the mesh resulted to be too coarse near the valves to properly capture them. This gave rise to numerical instabilities. Further developments of this work can be carried out in multiple directions. Refining the mesh could enable the use of physiological values for the valves thickness. Concerning the left ventricle movement, a displacement obtained from an electromechanical simulation that accounts for the restricted movement of the left ventricle can be integrated as input for the simulation of the aortic valve stenosis scenario.

References

[1] P. C. Africa. lifex: A flexible, high performance library for the numerical solution of complex finite element problems. *SoftwareX*, 20:101252, 2022.

[2] I. Avrahami, B. Even-Chen, and A. Liberzon. Hemodynamic effects of aortic valve and heart rate on coronary perfusion. *Clinical Biomechanics*, 78:105075, 2020.

[3] S. Di Gregorio, M. Fedele, G. Pontone, A. F. Corno, P. Zunino, C. Vergara, and A. Quarteroni. A computational model applied to myocardial perfusion in the human heart: from large coronaries to microvasculature. *Journal of Computational Physics*, 424:109836, 2021.

[4] A. Quarteroni, A. Manzoni, C. Vergara, and L. Dede'. *Mathematical modelling of the human cardiovascular system: data, numerical approximation, clinical applications*, volume 33. Cambridge University Press, 2019.

[5] A. Zingaro, C. Vergara, L. Dede', F. Regazzoni, and A. Quarteroni. A comprehensive mathematical model for cardiac perfusion. *Scientific Reports*, 13(1):14220, 2023.